

New test on General Relativity using galaxy-galaxy lensing with astronomical surveys

Zhaoting Chen,^{1,2,3,4} Wentao Luo,⁵ Yi-Fu Cai,^{1,2,3,*} and Emmanuel N. Saridakis^{1,6,†}

¹*Department of Astronomy, School of Physical Sciences,
University of Science and Technology of China, Hefei, Anhui 230026, China*

²*CAS Key Laboratory for Research in Galaxies and Cosmology,
University of Science and Technology of China, Hefei, Anhui 230026, China*

³*School of Astronomy and Space Science, University of Science and Technology of China, Hefei, Anhui 230026, China*

⁴*Jodrell Bank Centre for Astrophysics, Alan Turing Building,
School of Physics and Astronomy, The University of Manchester,
Oxford Road, Manchester, M13 9PL, United Kingdom*

⁵*Institute for the Physics and Mathematics of the Universe (Kavli IPMU, WPI), UTIAS,
Tokyo Institutes for Advanced Study, University of Tokyo, Chiba, 277-8583, Japan*

⁶*Department of Physics, National Technical University of Athens, Zografou Campus GR 157 73, Athens, Greece*

We use data from galaxy-galaxy weak lensing to perform a novel test on General Relativity (GR). In particular, we impose strong constraints using the torsional (teleparallel) formulation of gravity in which the deviation from GR is quantified by a single parameter α , an approximation which is always valid at low-redshift Universe and weak gravitational fields. We calculate the difference in the deflection angle and eventually derive the modified Excess Surface Density profile, which is mainly affected at small scales. Hence, confronting the predictions with weak lensing data from the Sloan Digital Sky Survey Data Release 7 we obtain the upper bound on the deviation parameter, which, expressed via the dimensionless percentage in the universe energy content, reads as $\log_{10}\Omega_\alpha \leq -18.52^{+0.80}_{-0.42}(\text{stat.})^{+1.50}_{-0.39}(\text{sys.})$ with systematics mainly arising from the modelling. To our knowledge, this is the first time that GR is verified at such an accuracy at the corresponding scales

PACS numbers: 98.80.-k, 04.80.Cc, 04.50.Kd, 98.80.Es

Introduction – As was initiated by Einstein over a century ago, investigations on the relation between gravitation and geometry provide insightful views on the nature of spacetime. Nevertheless, slight modifications from General Relativity (GR) have been proposed to explain cosmic acceleration at late and early times [1]. Such deviations from GR can be formulated either in the usual curvature formalism [2], or in the equivalent torsional (teleparallel) one [3]. Recently, it has become known that observations of the Large Scale Structure (LSS) of the Universe can be an effective probe to examine cosmological paradigms [4, 5]. Accordingly, it is suggested that a mild tension exists between the Cosmic Microwave Background (CMB) and LSS observations [6], hinting towards the possibility of a new theoretical framework beyond Λ -Cold-Dark-Matter (Λ CDM) cosmology or even beyond GR. Hence, it is interesting to explore GR and its alternatives in the context of LSS probes.

Measurements of gravitational lensing are very efficient towards such a direction. For instance, [7] uses gravitational lensing to test Emergent Gravity, while [8] studies the lensing potential around void regions based on the assumption of Cubic Galileon and Nonlocal gravity cosmologies. In particular, in this approach one typically considers a usual Schwarzschild geometry in the framework of GR and modifies the excess gravitational potential by introducing mass components that yield additional impacts on the Excess Surface Density (ESD) profile. Thus, it is natural to test theories of modified

gravity using weak lensing measurements in various experimental environments, such as void lensing [9], cluster formation and its density profile [10], cluster lensing [11, 12], etc. However, in most of pioneer studies the effective lensing potential has been treated as the average of two scalar potentials from the metric perturbation following the geodesic equation. Nevertheless, this fails to consider the geometric contribution to the local Euclidean definition of angle, which was first pointed out in [13], if one attempts to deal with no asymptotic flatness of Schwarzschild-de Sitter (SdS) spacetime.

In this Letter we use the new observational signatures on light-bending geometry to present an innovative test on GR, by using weak galaxy-galaxy lensing measurements. In particular, possible deviations from GR, quantified using the torsional formalism for convenience, alter the space-time geometry and thus affect the light bending [14]. Hence, with such an implication on light-bending geometry we show that the ESD profile at small scales can be sensitively affected, and thus, it is expected to be strictly constrained by astronomical observations. In order to illustrate the capability of this novel method, we make use of the galaxy group catalog and weak lensing shear catalog developed from the Sloan Digital Sky Survey (SDSS) Data Release (DR) 7, to rule out a class of deviations from GR.

Formalism – We begin with a brief discussion on torsional formulation of gravity following [3]. First of all, in this framework the (equivalent of) GR Lagrangian reads

as $\mathcal{L}_{GR} = T - 2\Lambda$, where Λ is the cosmological constant and T the torsion scalar that arises from contractions of the torsion tensor, similarly to the use of the Ricci scalar in GR. In a cosmic background of Friedmann-Lemaître-Robertson-Walker (FLRW) metric the torsion scalar becomes $T = -6H^2$, where H is the Hubble function, while for a spherically symmetry spacetime we acquire $T \propto r^{-2}$, where r is the radial coordinate. Hence, in the case of low-redshift Universe and weak gravitational fields that we focus in this study, any deviation from GR can be quantified as follows

$$f(T) = -2\Lambda + T + \alpha T^2 + \mathcal{O}(T^3), \quad (1)$$

where the parameter α has units of length squared.

It has been shown that for the theory (1) there exists a general class of spherically symmetric solutions $ds^2 = c^2 e^{A(r)} dt^2 - e^{B(r)} dr^2 - r^2 d\Omega$ of the form [14, 15]

$$\begin{aligned} A(r) &= -\frac{2GM}{c^2 r} - \frac{\Lambda}{3} r^2 - \frac{32\alpha}{r^2} \\ B(r) &= \frac{2GM}{c^2 r} + \frac{\Lambda}{3} r^2 + \frac{96\alpha}{r^2}, \end{aligned} \quad (2)$$

where we have neglected terms $\mathcal{O}(\alpha/r^2)^2$ due to the weak-field limit. As was expected, α quantifies the deviation of the usual Schwarzschild-de Sitter solution of GR. With this gravitational potential, the deflection angle at non-cosmological scales reads [14, 16]:

$$\hat{\beta} = 4GM/Rc^2 + 40\pi\alpha/R^2, \quad (3)$$

where R is the impact factor and M is the mass of the point source.

One could use relation (3) for confrontation with solar system data. However, such an application is inappropriate for the following considerations. Firstly, the modification to bending angle comparing to GR is independent of the source mass M and depends only on α . Hence, the point-mass approximation has to be strict, meaning that the impact factor must be much larger than the minimum radius which encloses most of point sources. Thus, application to lensing effects of the Sun, assuming that the mass enclosed within its radius can be viewed as a point-mass, is not consistent. Secondly, the Poisson equation for the Newtonian potential, which is used in weak lensing formalism to construct the relation between tangential shear and ESD profile, is no longer accurate. Under point-mass approximation, as we shall show later, the integrated average of ESD profile will encounter a divergence near $R = 0$, requiring us to introduce a cut-off radius. This is also a natural consequence of point-mass approximation. We emphasize that this does not imply nontrivial lensing under small R . In fact, when the field is strong the torsion scalar T reduces to $T = 2/r^2$, which is the case of teleparallel equivalent of GR.

On the other hand, in the context of galaxy-galaxy lensing the center can be modelled as a point-mass

source, given that the projected radius are well exceeding the scale that encloses most stellar mass component. This scale is typically much smaller than the scale of reconstructed ESD profile. Hence, in this regard the weak galaxy-galaxy lensing offers a better canvas for ruling out possible deviations from GR.

Weak lensing effects – The effective lensing potential $\psi(\vec{\xi})$ is defined as:

$$\psi(\vec{\xi}) = \frac{D_{ds}}{D_d D_s} \frac{2}{c^2} \int \Phi(\vec{\xi}, z) dz, \quad (4)$$

where $\vec{\xi}$ is the position on the lens plane and z is the comoving angular distance to lens plane, while D_{ds} , D_d , D_s are respectively the angular distances between lens and source, lens and observer, and observer and source. In GR this potential can be directly read from $A(r)$. However, since in deviations from GR depicted in (2) $A(r)$ and $B(r)$ have asymmetry, the lensing potential should be calculated via $\vec{\beta} = D_d \vec{\nabla}_\xi \psi$ (note that $\vec{\beta} = \frac{D_{ds}}{D_s} \vec{\beta}$). Although this does not provide a unique solution, it is expected that the physical solution should be $\Phi(1/r)$ without a constant. Hence, it leads to

$$\Phi(\vec{\xi}, z) = \Phi_{\text{Newton}} - 20 \frac{\alpha c^2}{r^2}, \quad (5)$$

with $r = (\xi^2 + z^2)^{1/2}$. Using the weak lensing formalism [17] we can calculate the convergence under the relation $\kappa(\xi) = D_d^2 \nabla_\xi^2 \psi / 2$ as

$$\kappa = \frac{4\pi G}{c^2} \frac{D_d D_{ds}}{D_s} \left[\Sigma(R) - \frac{10\alpha c^2}{GR^3} \right], \quad (6)$$

where Σ denotes the surface mass density. It is natural to define an effective surface mass density Σ_{eff} :

$$\Sigma_{\text{eff}} = \Sigma - \frac{10\alpha c^2}{GR^3}. \quad (7)$$

In order to acquire a more transparent picture of the physical meaning of this modification, we recall the relation between α and the critical density of the additional (torsional) energy component Ω_α^0 introduced by αT^2 , namely $\alpha = c^2 \Omega_\alpha^0 / (18H_0^2)$ [18–20].

As was discussed previously, for this modification to be applicable, the scale of projected radius much exceed the scale that encloses most of stellar mass component. As a reasonable consequence it is obvious that the modification diverges when averaging from 0 to the projected radius R , suggesting that a cut-off radius R_c should be imposed. Here we choose $R_c = R_{1/2}$, where $R_{1/2} \approx 0.015 R_{200}$ is the radius that encloses half of stellar mass (note that for a typical halo $M_{200} = 10^{12} M_\odot$ at $z = 0.1$, $R_c \sim 4\text{kpc}$), which has a universal linear relation to the virial radius of the galaxy [21]. Defining $\epsilon \equiv R_c/R$, then the modified ESD profile takes

$$\Delta \Sigma_{\text{eff}}(R) = \Delta \Sigma(R) + \frac{5c^4 \Omega_\alpha^0 (2 - \epsilon - \epsilon^2)}{9GH_0^2 R^3 \epsilon (1 + \epsilon)}. \quad (8)$$

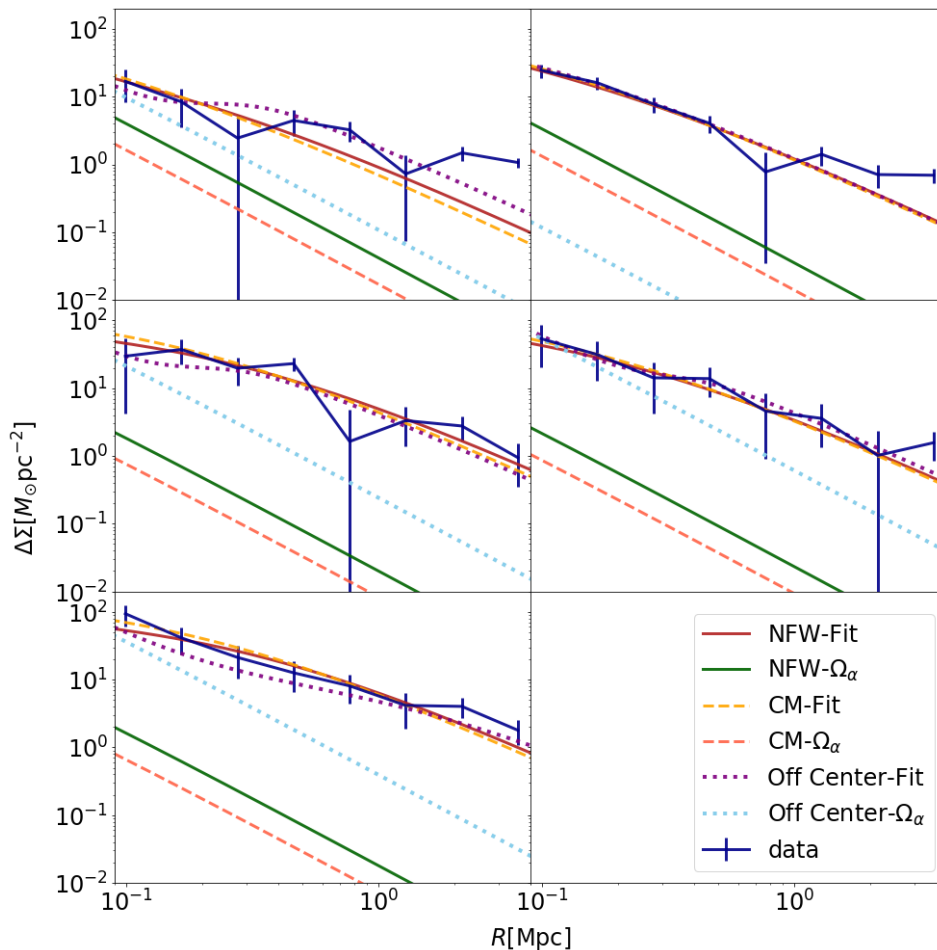


FIG. 1. The best-fit ESD profile. The horizontal axis is the projected distance away from the lens galaxy, while the vertical axis corresponds to lensing signals from the component and total ESD profiles. The data points are galaxy-galaxy lensing measurements around spectroscopic galaxies within different stellar mass bins. The errors are estimated based on bootstrap sampling. The overall fitted ESD is denoted with “-Fit” and contribution from beyond GR extension is denoted with “- Ω_α ”. Three different models, simple NFW with free concentration parameters (“NFW-”), simple NFW with fixed concentration-mass relation (“CM-”), NFW with off-center effect (“Off Center-”) are plotted as shown in the legends.

Hence, the effect of the induced modification due to the deviation from GR is

$$\Delta\Sigma_\alpha(R) \approx 2.3 \frac{M_\odot}{\text{pc}^2} \frac{\Omega_\alpha^0}{10^{-17}} \left(\frac{1\text{Mpc}}{R} \right)^2 \frac{1\text{kpc}}{R_c} \left(\frac{2 - \epsilon - \epsilon^2}{1 + \epsilon} \right). \quad (9)$$

We consider this effect to be a modification to the regular Λ CDM halo, which can be modelled as a NFW halo [22]. Accordingly, for consistency we require α , or equivalently Ω_α^0 , to be small so that the halo formation is not affected [23–26].

Results – We have now all the machinery to proceed to the confrontation of GR and its possible deviation with weak lensing data. We use data selected from group catalog built based on SDSS DR7 [27] in [28, 29]. The samples are then sub-divided into different stellar mass bin similar to [7]. We present detailed descriptions of this selection in the Appendix. The density profile can be modelled ac-

ording to [30], with the additional consideration of the off-center effect and stellar component.

Note that, in principle there exist mechanisms that can modify the NFW ESD profile within GR, such as the sub-halo contribution [31] to have similar effects on small scales. However, since we aim to demonstrate that Ω_α is severely constrained by weak lensing, we consider the following three scenarios to preliminarily extract the upper bound of the deviation parameter α . First, we use a simple NFW with α and treat halo mass and concentration as free parameters to demonstrate how an extremely small energy fraction of α can provide sizeable impact on small scales. Notice that, naturally because of the contribution, the concentration parameters are suppressed. Secondly, we adopt the concentration-mass relation (“CM-”) proposed in [32] to suppress the contribution from α , which tests the lower limit of our desired upper bound. Third, as a very conservative estimation,

we allow α to vary in different mass bins and adopt off-center effect (“Off Center-”) to further suppress the contribution from NFW halo on small scales, which tests the upper limit of our desired upper bound.

In Fig. 1 we present our fitting results. For each stellar mass bin, we set α to be an independent parameter for each fit, demonstrating the effect of $\Delta\Sigma_\alpha$. Since the typical R_c is much smaller than the smallest scale in the plot (~ 50 kpc), the contribution coming from $\Delta\Sigma_\alpha$ is a power law of R . As the data indicate, additional effects on small scales should lift the ESD profile, suggesting a positive α . Note that, for these five datasets the fitting for each scenario is roughly the same in terms of reduced χ^2 statistics. As we have expected, “CM-” fit gives a low amplitude of α , opposite to the “Off Center-” case. An intermediate fit of “NFW-” estimates a contribution of $\Delta\Sigma_\alpha \sim 10M_\odot\text{pc}^{-2}$ at scales smaller than 0.1 Mpc. This confirms that ESD on small scales is very sensitive to modified light bending beyond GR.

Then we estimate the upper bound for α . Following the argument above, we use the result of “NFW-” as our mean and statistical error. Theoretical systematics are estimated with “CM-” and “Off Center-”, with “CM-” provides a lower limit and the fourth stellar mass bin of “Off Center-” fit provides an upper limit. In summary, the upper bound of α is given by,

$$\alpha \leq 0.33_{-0.21}^{+1.76} \text{ pc}^2 ,$$

or equivalently:

$$\log_{10}\Omega_\alpha \leq -18.52_{-0.42}^{+0.80} , \quad (10)$$

at 68% confidence level with an estimation of systematic uncertainty of $_{-0.39}^{+1.50}$ from modelling. Hence, as we can see, the galaxy-galaxy weak lensing analysis implies that GR is verified to an order of $\sim 10^{-18}$, and any possible deviation beyond GR on galaxy scales should have this upper bound. This constraint is many orders of magnitude smaller than the corresponding one at the Solar System level [33, 34] ($\log_{10}\Omega_\alpha^0 \lesssim -10$).

As a self-consistency examination we estimate the quantity α/r^2 . In particular, at length scales of our data it becomes $\alpha/r^2 \sim 10^{-8}$, and thus the higher order terms were safely neglected from the solution (2) and the subsequent analyses. Additionally, we check whether the above upper bound on the deviation from GR is consistent with structure formation. An easy way to see this is by examining the modified Poisson equation for gravitational potential and matter overdensity at sub-horizon quasi-static approximation: $k^2\phi = 4\pi G_{\text{eff}}a^2\delta\rho$, in which the modification brought by beyond GR effect is $G_{\text{eff}}/G = 1/(1 + 2\alpha T/c^2)$ [35]. With the above bound on α we obtain $|1 - G_{\text{eff}}/G| \sim 10^{-19}$, and thus our analysis is consistent with the observed structure formation.

Viability. – As in previous analyses we made several assumptions and approximations, it is important to discuss

the viability of our results by examining the impact of each assumption and approximation. Firstly, the aforementioned choice of the cut-off radius R_c is conservative, and guarantees the robustness of our results. Note that, the bending geometry is based on two assumptions, i.e. spherical symmetry and weak field. We consider R_c which breaks the symmetry. Alternatively, taking R_c to break the weak field limit can also be considered. Currently we provide α at pc^2 level. In terms of the field strength, α/R_c^2 is very small, but if we take $\alpha/R_c^2 \sim 1$, then the characteristic scale of R_c will be much lower and the upper bound of $\log_{10}\Omega_\alpha$ will be around -20 . Thus, our claim of an upper bound on α is safe. Moreover, we further comment on the halo modeling effects. Here we consider a simple model to demonstrate the effect. However, our results still hold in a robust way, that even if all the ESD signals at low R are produced by α , such as the middle row of graphs of Fig. 1, then the upper bound of $\log_{10}\Omega_\alpha$ is ~ -17 , which remain extremely stringent. Additionally, uncertainties arising from the ESD signal reconstruction at small separations can yield a significant impact [36, 37]. Nevertheless, just as the halo modelling, unless the anticipated contribution from α is 10 times higher or lower than the present case, our results remain viable.

Conclusions. – In this Letter we apply the data from weak galaxy-galaxy lensing to test GR. To demonstrate the strong constraints upon deviations from GR, we particularly consider the torsional formulation of gravity by introducing a new deviation parameter α . By calculating the deflection angle in this modified gravity, we can derive the modified ESD profile, which is mainly affected at small scales. Therefore, confronting the theoretical predictions with weak lensing data from group catalog built based on SDSS DR7 [28, 29], we are able to extract the upper bound on α , which expressed through the dimensionless percentage in the universe energy content $\log_{10}\Omega_\alpha^0 \leq -18.16 \pm 0.63$. To our knowledge, this is for the first time that GR has been verified at such an accuracy at the aforementioned scales.

We conclude by highlighting the implications of the reported probe that can initiate several follow-up studies. We performed a novel weak galaxy-galaxy lensing test on GR. It is interesting to perform similar analyses to constraint cosmological scenarios beyond ΛCDM [38] or modifications such as $f(R)$ gravity [39]. As shown in this Letter, however, for extensions beyond GR which are of general validity at low-redshift universe and weak fields, quantified by a single parameter, we extracted very strict constraints. Phenomenologically, a crucial outcome is that, even for Infrared modifications of GR having cosmological implications at large scales, their Taylor expansions naturally generate high curvature/torsion terms that can be strongly bounded by the results reported in this Letter. On one hand, our analyses shed light on the motivation of theoretical investigations on possible

modifications to GR from fundamental theories yielding small deviations from GR. On the other hand, in the era of precision astronomy, a combination of various observational windows can impose tighter and tighter probes to GR and alternative theories.

Acknowledgments.— We are grateful to T. Qiu, M. Sasaki, P. Zhang and J. Zhu for valuable comments. This work is supported in part by the NSFC (No. 11722327, 11653002, 11961131007, 11421303, J1310021), by CAST Young Elite Scientists Sponsorship Program (2016QNR001), by the National Thousand Youth Talents Program of China, and by the Fundamental Research Funds for the Central Universities. ZC wishes to thank the Kavli IPMU for kind hospitality. WL acknowledges the support from WPI Japan. All numerics are operated on the computer clusters *Linda & Judy* in the particle cosmology group at USTC.

* yifucui@ustc.edu.cn

† msaridak@phys.uoa.gr

- [1] S. Capozziello and M. De Laurentis, Phys. Rept. **509**, 167 (2011) [[arXiv:1108.6266](#) [gr-qc]].
- [2] S. Nojiri and S. D. Odintsov, eConf C **0602061**, 06 (2006) [[hep-th/0601213](#)].
- [3] Y. F. Cai, S. Capozziello, M. De Laurentis and E. N. Saridakis, Rept. Prog. Phys. **79**, no. 10, 106901 (2016) [[arXiv:1511.07586](#) [gr-qc]].
- [4] E. van Uiteret *et al.*, Mon. Not. Roy. Astron. Soc. **476**, no. 4, 4662 (2018) [[arXiv:1706.05004](#) [astro-ph.CO]].
- [5] A. Spurio Mancini *et al.*, Mon. Not. Roy. Astron. Soc. **490**, no. 2, 2155 (2019) [[arXiv:1901.03686](#) [astro-ph.CO]].
- [6] M. Douspis, L. Salvati and N. Aghanim, PoS EDSU **2018**, 037 (2018) [[arXiv:1901.05289](#) [astro-ph.CO]].
- [7] M. M. Brouwer *et al.*, Mon. Not. Roy. Astron. Soc. **466**, no. 3, 2547 (2017) [[arXiv:1612.03034](#) [astro-ph.CO]].
- [8] A. Barreira, B. Li, E. Jennings, J. Merten, L. King, C. Baugh and S. Pascoli, Mon. Not. Roy. Astron. Soc. **454**, no. 4, 4085 (2015) [[arXiv:1505.03468](#) [astro-ph.CO]].
- [9] T. Baker, J. Clampitt, B. Jain and M. Trodden, Phys. Rev. D **98**, no. 2, 023511 (2018) [[arXiv:1803.07533](#) [astro-ph.CO]].
- [10] L. Lombriser, F. Schmidt, T. Baldauf, R. Mandelbaum, U. Seljak and R. E. Smith, Phys. Rev. D **85**, 102001 (2012) [[arXiv:1111.2020](#) [astro-ph.CO]].
- [11] T. Narikawa and K. Yamamoto, JCAP **1205**, 016 (2012) [[arXiv:1201.4037](#) [astro-ph.CO]].
- [12] T. Narikawa, T. Kobayashi, D. Yamauchi and R. Saito, Phys. Rev. D **87**, 124006 (2013) [[arXiv:1302.2311](#) [astro-ph.CO]].
- [13] W. Rindler and M. Ishak, Phys. Rev. D **76**, 043006 (2007) [[arXiv:0709.2948](#) [astro-ph]].
- [14] M. L. Ruggiero, Int. J. Mod. Phys. D **25**, no. 06, 1650073 (2016) [[arXiv:1601.00588](#) [gr-qc]].
- [15] G. Farrugia, J. L. Said and M. L. Ruggiero, Phys. Rev. D **93**, no. 10, 104034 (2016) [[arXiv:1605.07614](#) [gr-qc]].
- [16] L. M. Butcher, Phys. Rev. D **94**, no. 8, 083011 (2016) [[arXiv:1602.02751](#) [gr-qc]].
- [17] P. Schneider, [astro-ph/0509252](#).
- [18] S. Nesseris, S. Basilakos, E. N. Saridakis and L. Perivolaropoulos, Phys. Rev. D **88**, 103010 (2013) [[arXiv:1308.6142](#) [astro-ph.CO]].
- [19] S. Basilakos, S. Nesseris, F. K. Anagnostopoulos and E. N. Saridakis, JCAP **1808**, 008 (2018) [[arXiv:1803.09278](#) [astro-ph.CO]].
- [20] F. K. Anagnostopoulos, S. Basilakos and E. N. Saridakis, Phys. Rev. D **100**, no. 8, 083517 (2019) [[arXiv:1907.07533](#) [astro-ph.CO]].
- [21] A. V. Kravtsov, Astrophys. J. **764**, L31 (2013) [[arXiv:1212.2980](#) [astro-ph.CO]].
- [22] J. F. Navarro, C. S. Frenk and S. D. M. White, Astrophys. J. **490**, 493 (1997) [[astro-ph/9611107](#)].
- [23] Y. P. Wu and C. Q. Geng, JHEP **1211**, 142 (2012) [[arXiv:1211.1778](#) [gr-qc]].
- [24] A. Finch and J. L. Said, Eur. Phys. J. C **78**, no. 7, 560 (2018) [[arXiv:1806.09677](#) [astro-ph.GA]].
- [25] Y. F. Cai, M. Khurshudyan and E. N. Saridakis, Astrophys. J. **888**, 62 (2020) [[arXiv:1907.10813](#) [astro-ph.CO]].
- [26] S. Bahamonde, K. Flathmann and C. Pfeifer, Phys. Rev. D **100**, no. 8, 084064 (2019) [[arXiv:1907.10858](#) [gr-qc]].
- [27] K. N. Abazajian *et al.* [SDSS Collaboration], Astrophys. J. Suppl. **182**, 543 (2009) [[arXiv:0812.0649](#) [astro-ph]].
- [28] X. Yang, H. J. Mo, F. C. v. d. Bosch, A. Pasquali, C. Li and M. Barden, Astrophys. J. **671**, 153 (2007) [[arXiv:0707.4640](#) [astro-ph]].
- [29] W. Luo *et al.*, Astrophys. J. **836**, no. 1, 38 (2017) [[arXiv:1607.05406](#) [astro-ph.CO]].
- [30] C. O. Wright and T. G. Brainerd, Astrophys. J. **534**, 34 (1999), [[astro-ph/9908213](#)].
- [31] R. Mandelbaum, A. Tasitsiomi, U. Seljak, A. V. Kravtsov and R. H. Wechsler, Mon. Not. Roy. Astron. Soc. **362**, 1451 (2005) [[astro-ph/0410711](#)].
- [32] A. F. Neto *et al.*, Mon. Not. Roy. Astron. Soc. **381**, 1450 (2007) [[arXiv:0706.2919](#) [astro-ph]].
- [33] L. Iorio and E. N. Saridakis, Mon. Not. Roy. Astron. Soc. **427**, 1555 (2012) [[arXiv:1203.5781](#) [gr-qc]].
- [34] C. M. Will, Living Rev. Rel. **17**, 4 (2014) [[arXiv:1403.7377](#) [gr-qc]].
- [35] R. C. Nunes, JCAP **1805**, 052 (2018) [[arXiv:1802.02281](#) [gr-qc]].
- [36] A. Leauthaud *et al.*, Mon. Not. Roy. Astron. Soc. **467**, no. 3, 3024 (2017) [[arXiv:1611.08606](#) [astro-ph.CO]].
- [37] T. McClintock *et al.* [DES Collaboration], Mon. Not. Roy. Astron. Soc. **482**, no. 1, 1352 (2019) [[arXiv:1805.00039](#) [astro-ph.CO]].
- [38] J. Zhang, R. An, W. Luo, Z. Li, S. Liao and B. Wang, Astrophys. J. **875**, no. 2, L11 (2019) [[arXiv:1807.05522](#) [astro-ph.CO]].
- [39] B. Li and M. Shirasaki, Mon. Not. Roy. Astron. Soc. **474**, no. 3, 3599 (2018) [[arXiv:1710.07291](#) [astro-ph.CO]].
- [40] E. F. Bell, D. H. McIntosh, N. Katz and M. D. Weinberg, Astrophys. J. Suppl. **149**, 289 (2003) [[astro-ph/0302543](#)].
- [41] C. M. Hirata and U. Seljak, Mon. Not. Roy. Astron. Soc. **343**, 459 (2003) [[astro-ph/0301054](#)].
- [42] R. Mandelbaum *et al.*, Mon. Not. Roy. Astron. Soc. **361**, 1287 (2005) [[astro-ph/0501201](#)].
- [43] M. R. George *et al.*, Astrophys. J. **757**, 2 (2012) [[arXiv:1205.4262](#) [astro-ph.CO]].
- [44] U. Seljak and M. S. Warren, Mon. Not. Roy. Astron. Soc. **355**, 129 (2004) [[astro-ph/0403698](#)].
- [45] W. Luo *et al.*, Astrophys. J. **862**, no. 1, 4 (2018) [[arXiv:1712.09030](#) [astro-ph.CO]].
- [46] D. E. Johnston, E. S. Sheldon, A. Tasitsiomi, J. A. Frie-

man, R. H. Wechsler and T. A. McKay, *Astrophys. J.* **656**, 27-41 (2007) doi:10.1086/510060 [arXiv:astro-ph/0507467 [astro-ph]].

Appendix

Lenses.— The lenses are from group catalog built based on SDSS DR7 [28], namely 472419 groups out of which 368020 are with halo mass estimation based on abundance matching. In order to minimize the effects of nearby structures we only select single galaxy systems which further reduce the number to 326172. All the sizes of those single galaxy systems are quantified by virial radius, which is the radius containing 180 overdensity compared to the mean density of the universe. There are 36,759 galaxies which have no spectroscopic redshift due to fiber collision, yet assigned to the redshift of their nearby galaxies. Those galaxies are included in the group-finding procedure, and thus the single systems are not effected by the fiber collision effect.

The samples are sub-divided into different stellar mass bins, similar to [7], while increasing the number of samples and including a higher stellar mass bin. The stellar mass of this sample is estimated based on [40]. The basic statistical properties of the binning of the sample are given in Table I.

$\log_{10} M_{st}$ range	N_{sat}	$\langle z \rangle$	$\langle \log_{10} M_{st} \rangle$	$\langle \log_{10} M_h \rangle$
8.5-10.5	145 298	0.091	10.266	11.995
10.5-10.8	104 773	0.123	10.648	12.441
10.8-10.9	28 833	0.143	10.848	12.748
10.9-11.0	22 427	0.155	10.946	12.922
11.0-11.8	24 841	0.165	11.087	13.237

TABLE I. Properties of the lens samples created for this Letter.

Sources.— The source catalog based on SDSS DR7 is from [29]. The Excess Surface Density (ESD) is related to the stacked shape by the geometry factor Σ_{cr} through $\gamma_T(R)\Sigma_{cr} = \Delta\Sigma(R)$. Instead of measuring γ_T , it is more convenient to directly measure $\Delta\Sigma(R)$ as a whole by applying both photometric and spectroscopic redshift so that

$$\Delta\Sigma(R) = \frac{1}{2\mathcal{R}} \frac{\sum_{l,s} w_{l,s} e_{t,ls} [\Sigma_{cr,ls}^{-1}]^{-1}}{\sum_{l,s} w_{l,s}}. \quad (11)$$

\mathcal{R} is the responsivity of shear given a shape estimator, and we use a universal shear responsivity by using the shape distribution of the source sample that $\mathcal{R} = 1 - \sum_{l,s} e_{rms}^2 w_{l,s} / \sum_{l,s} w_{l,s}$. The weight contains not only shape noise and measurement error, but additionally the

geometry factor Σ_{cr} , namely $w_{l,s} = (\Sigma_{cr,ls}^{-1})^2 / (\sigma_e^2 + e_{rms}^2)$, where σ_e is the shape noise and e_{rms} is the error caused by the sky background noise and Poisson noise of each galaxy. Finally, l, s denotes each lens-source pair system.

The major systematics arise from photometric redshift error [41, 42], which can lead up to 3% systematic errors in lensing measurements. Moreover, we apply the boost factor to account for the other contamination caused by photometric error, which leads to misidentification of low- z galaxies as high- z galaxies. The boost factor is actually the ratio between the number of galaxies within radius for the lens sample and random points of a survey $B(r) = n(R)/n_{rand}(R)$, and therefore the final measured ESD is multiplied by this factor.

NFW halo.— The ESD of a dark matter halo is typically modelled as an NFW halo [30] with off-center effect. The NFW halo profile consists of two parameters, the characteristic mass scale M_{200} and the concentration c . We adopt the following concentration-mass relation to reduce the degree of freedom [32]: $c = 4.67(M_{200}/10^{14}h^{-1}M_{\odot})^{-0.11}$. The total ESD is a sum of several component:

$$\Delta\Sigma(R) = \Delta\Sigma_{\text{host}} + \Delta\Sigma_{\text{sub}} + \Delta\Sigma_{*} + \Delta\Sigma_{2h}, \quad (12)$$

where host halo, satellite halo, stars and two-halo component are included. For a single off-center radius R_{off} , the ESD profile changes to [46]:

$$\Sigma(R|R_{\text{off}}) = \frac{1}{2\pi} \int_0^{2\pi} \Sigma_{\text{NFW}}(\sqrt{R^2 + R_{\text{off}}^2 + 2R_{\text{off}}R \cos \theta}) d\theta, \quad (13)$$

while the actual ESD profile of the host halo is the convolution between the off-center radius and $\Sigma(R|R_{\text{off}})$, i.e. $\Sigma_{\text{host}} = \int dR_{\text{off}} P(R_{\text{off}}) \Sigma(R|R_{\text{off}})$, where $P(R_{\text{off}}) = \exp[-(R_{\text{off}}/R_{\text{sig}})^2/2] R_{\text{off}}/R_{\text{sig}}^2$. For $\Delta\Sigma_{*}$, the stellar mass component can be simply treated as a point-mass [43], namely $\Delta\Sigma_{*}(R) = M_{*}/(2\pi R^2)$, where M_{*} is the stellar mass of candidate central galaxy.

The 2-halo term can be calculated through the halo-matter correlation function [44]. As shown in [45], the 2-halo term remains trivially small below the scale of 1 Mpc and becomes significant at larger scales. Thus, for the first two stellar mass bins used in our data, we have neglected the largest R when fitting the ESD since at that scale the measured $\Delta\Sigma$ is below $1 M_{\odot}/\text{pc}^2$.

There is some possibility that the candidate lens galaxy is not the true central galaxy and may contain the sub-halo component. In addition, in the group finder, there are some possibilities that the central galaxy is an interloper and may contain its original host halo component. Hence, usually a sub-halo component $\Delta\Sigma_{\text{sub}}$ will be included. However, as this component also affects mainly the small scales, introducing it leads to degeneracy between $\Delta\Sigma_{\alpha}$ and $\Delta\Sigma_{\text{sub}}$. Thus, we neglect this term for our modeling and we deduce that this estimation is the upper bound of α .